



## OPEN AI-based analysis of surgical outcomes in vitrectomy with and without cystotomy for refractory cystoid diabetic macular edema

Mizuho Mitamura, Michiyuki Saito✉, Kiriko Nishiyama-Hirooka, Zhenyu Dong, Ryo Ando, Satoru Kase & Susumu Ishida

The aim of this study was to compare surgical outcomes in vitrectomy with and without cystotomy for refractory cystoid diabetic macular edema (DME). This study enrolled 35 eyes of 29 patients who underwent vitrectomy for refractory DME. The eyes were divided into 2 groups, those undergoing vitrectomy with cystotomy (cystotomy group) ( $n=8$ ) and vitrectomy with internal limiting membrane (ILM) peeling only (ILM peeling group) ( $n=27$ ). The endpoints were central retinal thickness (CRT), best-corrected visual acuity (BCVA), macular fluid (MF) area. The MF area was determined and measured using a semantic segmentation model “Hokkaido University MF segmentation model” and subdivided into inner MF (IMF) area bounded by the inner nuclear layer (INL), and outer MF (OMF) area between the outer border of INL and ellipsoid zone. The cystotomy group showed a significant reduction in CRT at 1 month postoperatively compared to the ILM peeling group ( $P<0.05$ ). The cystotomy group preserved BCVA at 6 months postoperatively compared to preoperatively. There was a significant difference between the cystotomy and the ILM peeling groups in the reduction of the OMF area at 1 month postoperatively ( $P<0.01$ ). Cystotomy for refractory DME was more effective in reducing the OMF area.

**Keywords** Diabetic macular edema, Pars plana vitrectomy, Cystotomy, Artificial intelligence

### Abbreviations

DME	Diabetic macular edema
ILM	Internal limiting membrane
CRT	Central retinal thickness
BCVA	Best-corrected visual acuity
MF	Macular fluid
IMF	Inner MF
OMF	Outer MF
VEGF	Vascular endothelial growth factor
INL	Inner nuclear layer
OCT	Optical coherence tomography
EZ	Ellipsoid zone
AI	Artificial intelligence
FP	False-positive
FN	False-negative
TP	True-positive
TN	True-negative
AUC	Area under the receiver operating characteristic curve
ERM	Epiretinal membrane
STTA	Sub-Tenon injection of triamcinolone acetonide
ANOVA	Analysis of variance

Department of Ophthalmology, Faculty of Medicine, Graduate School of Medicine, Hokkaido University, N-15, W-7, Kita-ku, Sapporo 060-8638, Japan. ✉email: s.michiyuki@med.hokudai.ac.jp

Diabetic macular edema (DME) is one of the most common causes of vision loss in diabetic patients in developed countries<sup>1</sup>. There are several treatment approaches for DME, including focal macular photocoagulation and intravitreal injections of steroids and/or anti-vascular endothelial growth factor (VEGF) agents<sup>2–5</sup>. In recent years, anti-VEGF drugs have shown spectacular therapeutic effects. Still, vitrectomy may be effective for DME that is poorly controlled even with local and medical treatments<sup>6,7</sup>. There are two possible mechanisms by which vitrectomy contributes to the treatment of refractory DME. One is the release of vitreous adhesions on the macular surface. The removal of vitreous traction physically reduces macular edema<sup>8</sup>. The second is the improvement of clearance in the vitreous cavity by replacing the vitreous gel with liquid. This is expected to reduce the concentration of VEGF in the vitreous cavity by removing inflammatory cells and cytokines<sup>9,10</sup>.

However, cases with DME recurrence were experienced even with no vitreous itself and no vitreous traction after vitrectomy, suggesting that a more direct approach to DME resolution may be practical. Tachi N et al. were the first to report a direct approach to eliminate the macular cysts by several methods, including puncture and aspiration of the fluid, an incision or excision of the cyst wall, and lateral puncture with a subretinal canula through the retina<sup>11</sup>. The retrospective observational study of 30 eyes showed significant improvement in central retinal thickness (CRT) and best-corrected visual acuity (BCVA) 12 months after surgery compared to preoperatively<sup>12</sup>. The prospective, interventional study of 20 eyes in 18 patients showed significant improvement in postoperative CRT and BCVA, which might be more effective than conventional vitrectomy with internal limiting membrane (ILM) peeling<sup>13</sup>.

However, to the best of our knowledge, there have been no studies comparing the surgical outcomes of vitrectomy including detailed analysis of cyst area and other clinical characteristics with and without cystotomy for refractory cystoid DME. In this study, we compared surgical outcomes of the eyes of DME patients between 2 groups who underwent vitrectomy with cystotomy and those who underwent vitrectomy with ILM peeling but without cystotomy.

## Results

### Clinical background

Table 1 shows the clinical background in this study. Eight eyes in 8 patients (5 males and 3 females) were in the cystotomy group and 27 eyes in 23 patients (15 males and 8 females) were in the ILM peeling group. In the cystotomy group, the mean age at surgery was  $66.8 \pm 8.2$  years (range 54–78 years). Preoperatively, 2 eyes were pseudophakic and 6 eyes were phakic. In all phakic eyes, phacoemulsification and intraocular lens implantation were performed at the same time of surgery for DME. One case with epiretinal membrane (ERM) underwent ERM peeling. In the ILM peeling group, mean age at surgery was  $65.3 \pm 7.4$  years (range 52–81 years). In 22 patients, phacoemulsification and intraocular lens implantation were performed simultaneously with pars plana vitrectomy, and 5 patients underwent vitrectomy only. Fifteen cases with ERM underwent ERM peeling. There were no significant differences in age, sex, or the number of patients receiving combined cataract surgery. Preoperative complication of ERM was higher in the ILM peeling group than in the cystotomy group.

### CRT values

As shown in Fig. 1, CRT in the cystotomy group versus (vs.) the ILM peeling group was  $659.5 \pm 318.4$  vs.  $571.2 \pm 150.7$   $\mu\text{m}$  preoperatively ( $P=0.80$ ),  $251.5 \pm 181.6$  vs.  $402.92 \pm 156.4$   $\mu\text{m}$  1 month after surgery ( $P=0.017$ ),  $274.3 \pm 191.6$  vs.  $353.0 \pm 142.9$   $\mu\text{m}$  3 months after surgery ( $P=0.14$ ), and  $283.6 \pm 178.3$  vs.  $363.8 \pm 208.9$   $\mu\text{m}$  at 6 months ( $P=0.40$ ). The cystotomy group showed a significant decrease in CRT 1 month after surgery compared to the ILM peeling group, but there was no significant difference preoperatively, or at 3, and 6 months postoperatively. Both the cystotomy group and ILM peeling group showed a significant decrease in CRT at 1, 3, 6 months postoperatively compared to preoperatively (cystotomy group:  $P=0.023$ ,  $P=0.055$ ,  $P=0.031$ ; ILM peeling group:  $P=0.022$ ,  $P<0.0001$ ,  $P=0.0013$ ; respectively). Analysis of variance (ANOVA) with CRT as the dependent variable, and postoperative time period and cystotomy as independent variables showed that CRT was significantly affected by cystotomy ( $F(1, 33)=5.31$ ,  $P=0.023$ ) and postoperative time period ( $F(1, 33)=17.8$ ,  $P<0.0001$ ).

### LogMAR BCVA

As shown in Fig. 2, logMAR BCVA in the cystotomy group vs. ILM peeling group was  $0.76 \pm 0.28$  vs.  $0.75 \pm 0.31$  preoperatively ( $P=0.97$ ),  $0.78 \pm 0.32$  vs.  $0.77 \pm 0.43$  at 1 month ( $P=0.84$ ),  $0.75 \pm 0.23$  vs.  $0.71 \pm 0.45$  at 3 months ( $P=0.72$ ) and  $0.72 \pm 0.27$  vs.  $0.80 \pm 0.50$  at 6 months after surgery ( $P=1$ ). There was no significant difference in logMAR BCVA for the entire postoperative period (1, 3, 6 months) compared to preoperatively in either the

	Cystotomy group	ILM peeling group	P value
Number of eyes	8	27	-
Number of patients	8	23	-
Male/Female ratio	5/3	15/8	$P=1.0$
Age at surgery (years)	$66.8 \pm 8.21$	$65.3 \pm 7.36$	$P=0.62$
Cataract surgery with vitrectomy	6	22	$P=0.64$
Complication of ERM	1	15	$P=0.02$

**Table 1.** Clinical characteristics in the cystotomy group and the ILM peeling group. ERM, epiretinal membrane; Fisher's exact test; T-test.

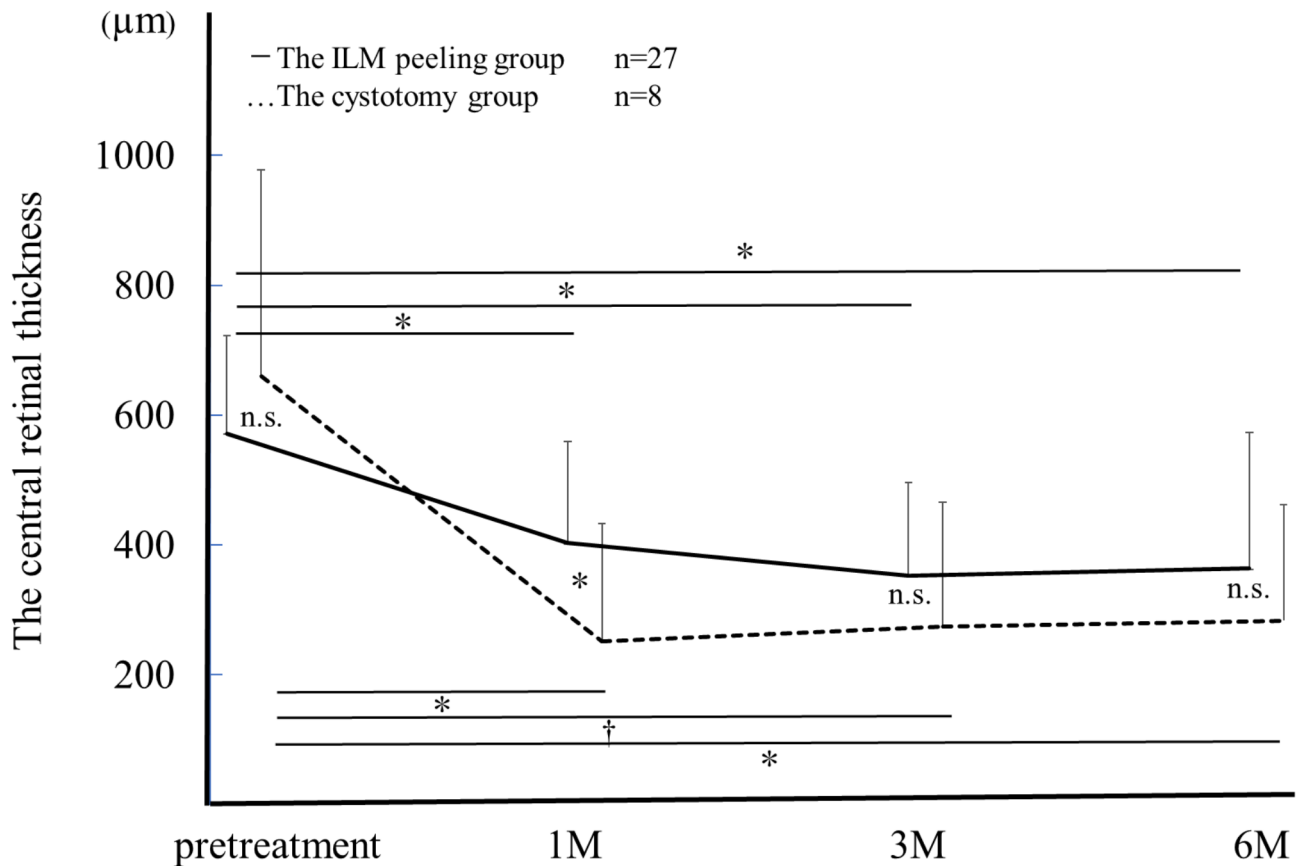


**Fig. 1.** Changes in the central retinal thickness at preoperatively and 1, 3, and 6 months postoperatively in the cystotomy groups vs. the ILM peeling groups. n.s.: not significant, \* $P < 0.05$ , † $P < 0.1$ , Mann-Whitney U test for comparison between groups and Wilcoxon signed-rank test for comparison of time periods in each group.

cystotomy group or ILM peeling group (cystotomy group:  $P = 1.0$ ,  $P = 0.91$ ,  $P = 0.70$ ; ILM peeling group:  $P = 0.98$ ,  $P = 0.67$ ,  $P = 0.97$ ; respectively).

#### The macular fluid (MF) area

The analysis for MF area was performed in 8 eyes in the cystotomy group and 19 eyes in the ILM peeling group, where the quality of OCT images were sufficient for AI-based semantic segmentation. In a representative case of the cystotomy group, a large cyst was found in the outer retina preoperatively (Fig. 3A). After the cystotomy was performed, both inner MF (IMF) and outer MF (OMF) areas measured by AI at 1 and 3 months postoperatively decreased (Fig. 3B and C), but there was a recurrence at 6 months postoperatively (Fig. 3D). In a representative case of the ILM peeling group, there were prominent edematous lesions in the inner retina with ERM (Fig. 3E). At 1, 3, and 6 months postoperatively, both IMF and in OMF areas decreased (Fig. 3F, G, and H).

As shown in Fig. 4, the IMF area in the cystotomy group vs. ILM peeling group was  $426 \pm 538$  vs.  $777 \pm 1005$  pixels preoperatively ( $P = 0.61$ ),  $147 \pm 274$  vs.  $229 \pm 560$  pixels 1 month after surgery ( $P = 0.36$ ),  $179 \pm 184$  vs.  $482 \pm 593$  pixels 3 months after surgery ( $P = 0.71$ ), and  $894 \pm 1443$  vs.  $992 \pm 2224$  pixels at 6 months ( $P = 0.44$ ). There was no significant difference between the two groups at each time point. There was no significant difference in IMF area for the entire postoperative period (1, 3, 6 months) compared to preoperatively in the cystotomy group, but a significant decrease at 1 month postoperatively compared to preoperatively in the ILM peeling group (cystotomy group:  $P = 0.06$ ,  $P = 0.21$ ,  $P = 0.59$ ; ILM peeling group:  $P = 0.01$ ,  $P = 0.37$ ,  $P = 1.0$ ; respectively). Due to the wide individual differences among patients, ANOVA were performed using the difference from the preoperative value as a correction value. ANOVA with the IMF area as the dependent variable, and postoperative period and cystotomy as independent variables showed that the IMF area was significantly affected by postoperative period ( $F(1, 25) = 5.176$ ,  $P = 0.0258$ ).

As shown in Fig. 5, the OMF area in the cystotomy group vs. ILM peeling group was  $6451 \pm 1925$  vs.  $4501 \pm 5104$  pixels preoperatively ( $P = 0.0096$ ),  $1445 \pm 1875$  vs.  $3281 \pm 4756$  pixels 1 month after surgery ( $P = 0.81$ ),  $2192 \pm 2398$  vs.  $2794 \pm 3220$  pixels 3 months after surgery ( $P = 0.56$ ), and  $1802 \pm 2068$  vs.  $3803 \pm 6617$  pixels at 6 months ( $P = 0.49$ ). There was a significant difference between the two groups preoperatively. In the cystotomy group, there was a significant decrease between preoperatively and 1, 3, and 6 months after surgery ( $P = 0.016$ ,  $P = 0.03$ ,  $P = 0.016$ ; respectively). There was no significant difference in OMF area for the entire postoperative period (1, 3, 6 months) compared to preoperatively in the ILM peeling group ( $P = 0.31$ ,  $P = 0.21$ ,  $P = 0.35$ ; respectively). ANOVA with the OMF area as the dependent variable, and postoperative time and cystotomy

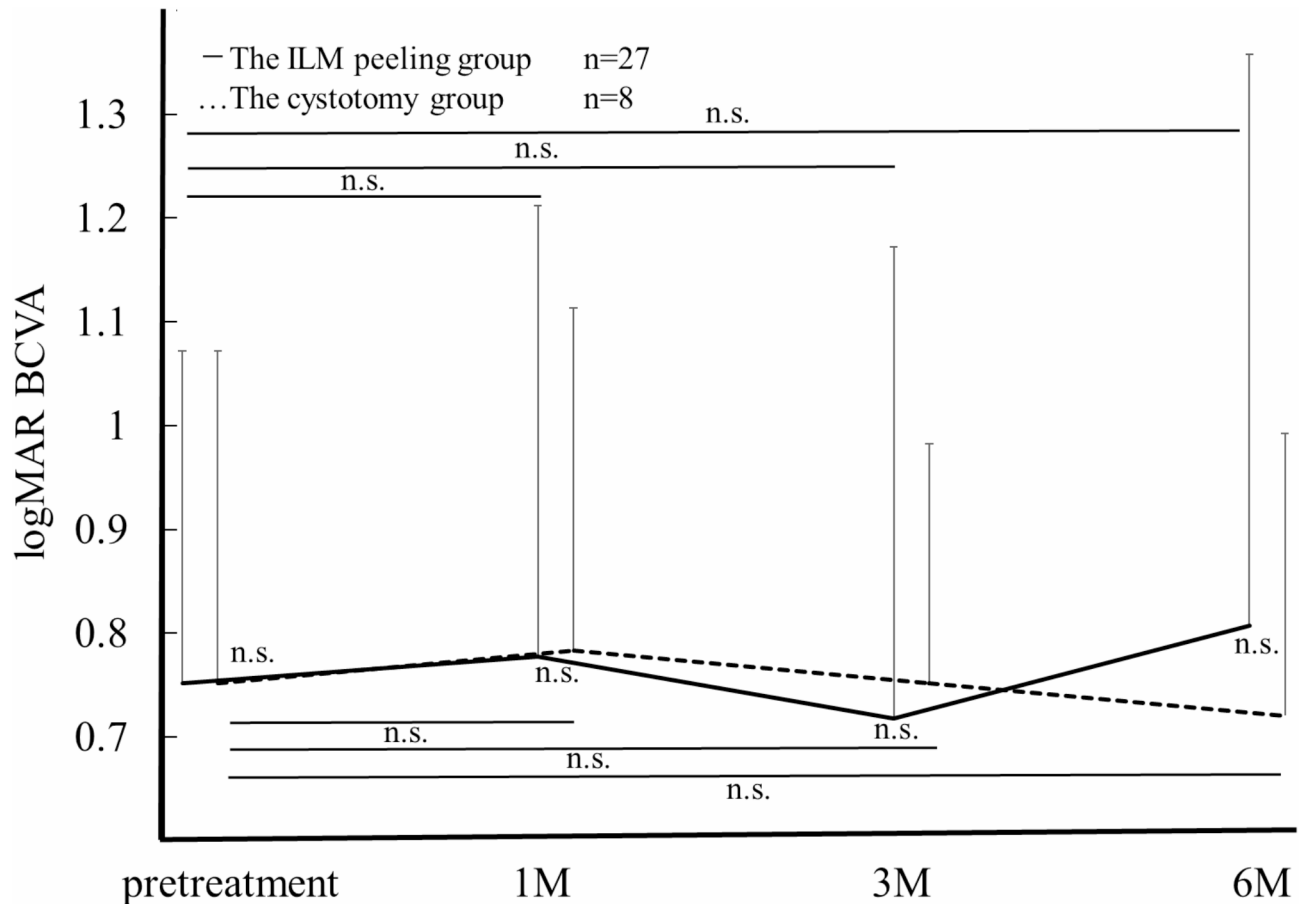


**Fig. 2.** Changes in the logMAR best-corrected visual acuity (BCVA) at preoperatively and 1, 3, and 6 months postoperatively in the cystotomy groups vs. the ILM peeling groups. n.s.: not significant, Mann-Whitney U test for comparison between groups and Wilcoxon signed-rank test for comparison of time periods in each group.

as independent variables showed that the OMF area was significantly affected by cystotomy ( $F(1, 25) = 4.364$ ,  $P = 0.0401$ ).

### The total number of intravitreal injections with anti-VEGF agents and sub-Tenon injection of triamcinolone acetonide (STTA) preoperatively and during the 6-month postoperative period

The total number of anti-VEGF agents administered preoperatively was higher in the cystotomy group ( $5.1 \pm 5.7$ ) than in ILM peeling group ( $0.3 \pm 0.8$ ) ( $P < 0.0001$ ). The total number of preoperative STTA was not significantly different, i.e.,  $1.5 \pm 1.9$  vs.  $0.7 \pm 1.3$  in the cystotomy group vs. ILM peeling group ( $P = 0.20$ ). The number of anti-VEGF agents administered during the 6-month postoperative period was not significantly different, i.e.,  $0.1 \pm 0.1$  vs.  $0.6 \pm 2.7$  in the cystotomy group vs. ILM peeling group ( $P = 0.43$ ). The number of STTA during the 6-month postoperative period was not significantly different, i.e.,  $0.3 \pm 0.5$  vs.  $0.6 \pm 1.3$  in the cystotomy group vs. ILM peeling group ( $P = 0.38$ ).

### Discussion

This study showed important findings on vitrectomy with cystotomy for refractory cystoid DME as follows: (1) the cystotomy group showed a significant reduction in CRT 1 month after surgery compared to the ILM peeling group, and cystotomy was a significant factor for reducing postoperative CRT, (2) the MF area especially the OMF area in the cystotomy group showed a significant decrease between preoperatively and postoperatively, and cystotomy was a significant factor for affecting OMF area.

In the present study, the cystotomy group showed a significant reduction in CRT as early as 1 month postoperatively compared to the ILM peeling group, and cystotomy was a significant factor that reduced CRT. DME presents with vascular leakage due to disruption of the inner blood-retinal barrier and increase of inflammatory cytokines<sup>14,15</sup>. Fluid accumulation in the outer and inner retinal layers leads to retinal thickening, and prolonged DME causes irreversible photoreceptor dysfunction<sup>16</sup>. Early postoperative reduction in CRT after cystotomy for refractory cystoid DME may help preserve visual function in the long term.

Furthermore, we analyzed the MF area which was subdivided into the IMF and OMF areas using AI. There are two advantages of using semantic segmentation technology to detect MF. The first advantage is that it automatically calculates the detailed area of MFs as a probability map that is difficult and bothersome for

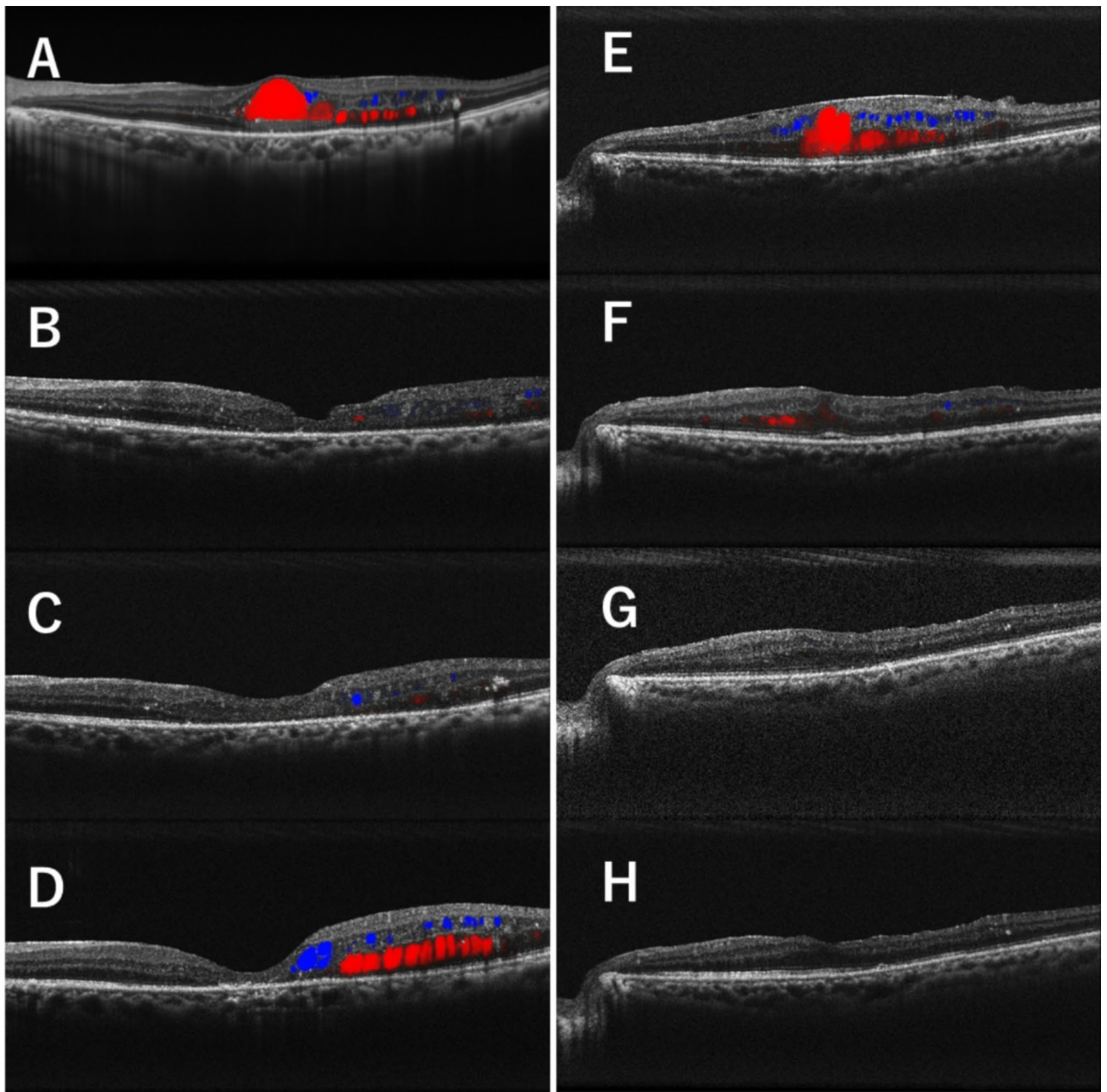


**Fig. 3.** Macular fluid (MF) area measurement on the horizontal scans of the swept-source optical coherence tomography image in the representative case of the cystotomy group (A ~ D) and of the internal limiting membrane (ILM) peeling group (E ~ H). A The representative case of the cystotomy group shows a large cyst in the outer retina preoperatively. The blue area shows the inner MF (IMF) area, and the red area shows the outer MF (OMF) area. B One month after vitrectomy surgery with cystotomy. C Three months after surgery. D Six months after surgery. E The representative case of the ILM peeling group shows multiple edematous lesions in the inner retina with the epiretinal membrane. F One month after vitrectomy surgery with ILM peeling only. G Three months after surgery. H Six months after surgery.

humans to draw. The second is that the AI learns and standardizes from learning data and excludes the observer biases that can arise when humans perform such a detailed measurement. The IMF area showed a significant decrease at one month postoperatively in the ILM peeling group; and, the postoperative period contribute to changes of the IMF area regardless of the presence or absence of cystotomy. Regarding the similar changes in the MFs in both groups, it was possible that the changes were caused by the common therapeutic mechanisms, i.e., release of vitreous traction and/or improvement of vitreous clearance due to vitrectomy and ILM peeling technique, common procedures for both groups. On the other hand, the OMF area, especially in the cystotomy group, showed a significant decrease between preoperatively and postoperatively, and the addition of cystotomy significantly contributed to the reduction. Histopathological studies have reported that cystoid edema in DME

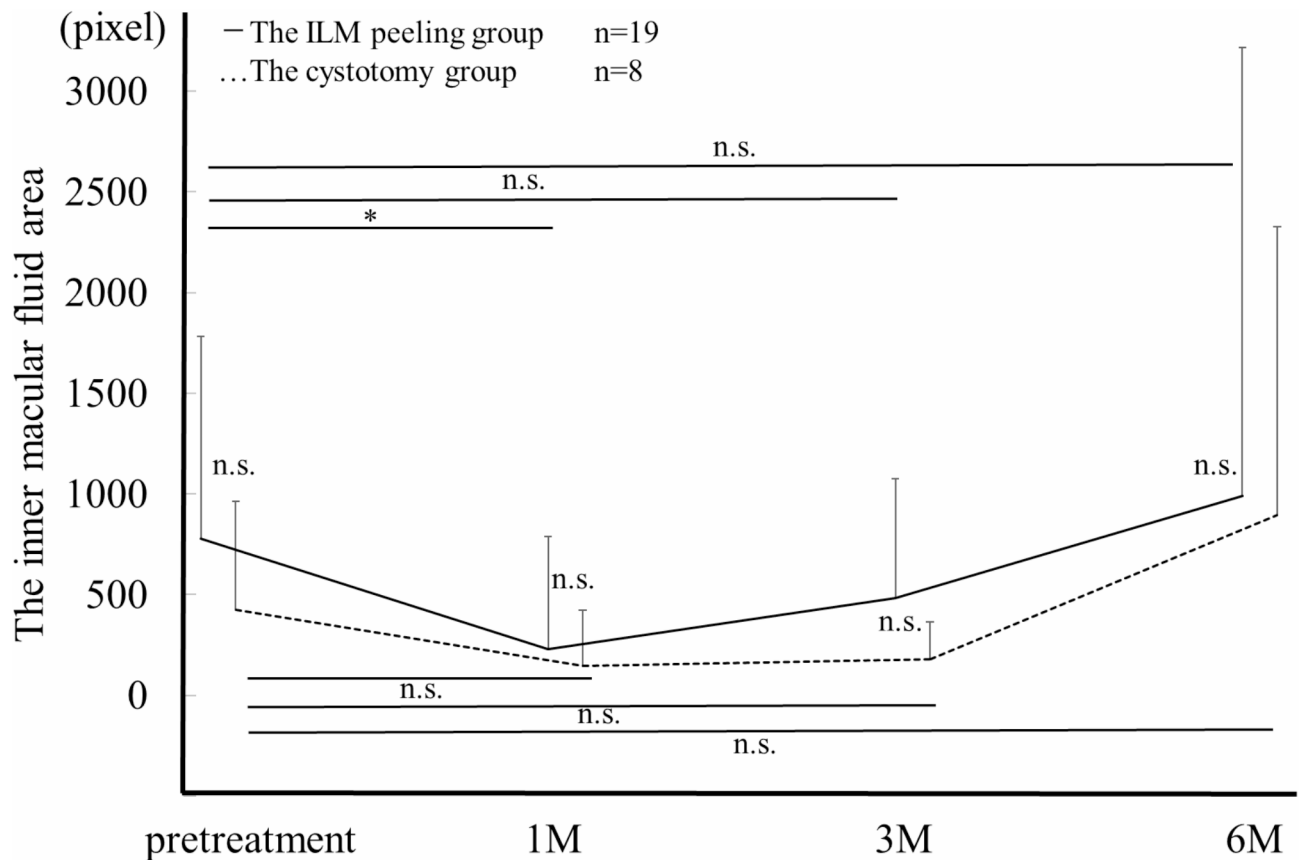


**Fig. 4.** Changes in the area of inner macular fluid at preoperatively and 1, 3, and 6 months postoperatively in the cystotomy group vs. the ILM peeling group. n.s.: not significant, \* $P < 0.05$ , Mann-Whitney U test for comparison between groups and Wilcoxon signed-rank test for comparison of time periods in each group.

occurs mainly in the inner nuclear layer (INL), outer plexiform layer, and Henle fiber layer<sup>17</sup>. Therefore, large cysts at the fovea are present in the outer plexiform layer and Henle fiber layer. In this study, especially in the cystotomy group, the OMF area before surgery was basically large as shown in Fig. 3, leading to the apparent effect of the cystotomy on the reduction.

The therapeutic mechanisms of conventional vitrectomy for DME are thought to be the relaxation of vitreomacular traction and the decrease of VEGF concentration in the vitreous cavity due to the improvement of vitreous clearance<sup>8–10</sup>. The result of this study showed the postoperative alteration of MF was different between the IMF and OMF areas, suggesting that cystotomy has a different treatment mechanism on top of conventional vitrectomy. Reasonably, this study clarified the distinct pattern of OMF-selective response after cystotomy. There have been two previous reports on cyst contents. Imai H et al. analyzed DME cyst contents by mass spectrometry and reported that the structure was composed of fibrinogen<sup>18</sup>. We have recently shown by immunohistochemistry that the excised cyst specimen was fibrin/fibrinogen modified with advanced glycation end-products<sup>19</sup>. The first mechanism of cystotomy, based on these findings, is that fibrin-rich contents with pro-inflammatory substances are released into the vitreous cavity by cystotomy, which changes the osmotic pressure and inhibits serous retention. The second mechanism is that physically removing the upper wall of the cyst causes an outflow path to the vitreous cavity, which maintains cyst resolution.

In our study, the mean BCVA of the cystotomy group were preserved 6 months after surgery ( $0.72 \pm 0.27$ ) compared to preoperatively ( $0.76 \pm 0.28$ ). There have been 2 previous reports on visual acuity changes following the cystotomy as follows: the retrospective observational study of 30 eyes showed significant improvement in BCVA from  $0.45 \pm 0.33$  preoperatively to  $0.33 \pm 0.25$  1 year after surgery<sup>12</sup>. In the prospective intervention study of 20 eyes in 18 patients, BCVA showed significant improvement from  $0.43 \pm 0.31$  preoperatively to  $0.25 \pm 0.23$  6 months after surgery<sup>13</sup>. The patients in our study had a lower BCVA at the time of surgical intervention than those previously reported and included patients with irreversible ellipsoid zone (EZ) impairment, resulting in a small improvement in BCVA. Long-term visual prognosis and the timing of treatment interventions need to be investigated by further studies.

Additionally, the total number of anti-VEGF injections in the cystotomy group was higher preoperatively and lower postoperatively than that in the ILM peeling group. This implies a potential benefit to patients in terms of reducing the number of hospital visits and the amounts of healthcare costs.

This study has some limitations. First, this study was retrospective, and details of surgical technique, timing and duration of follow-up, and preoperative treatment differed among surgeons, resulting in a selection bias

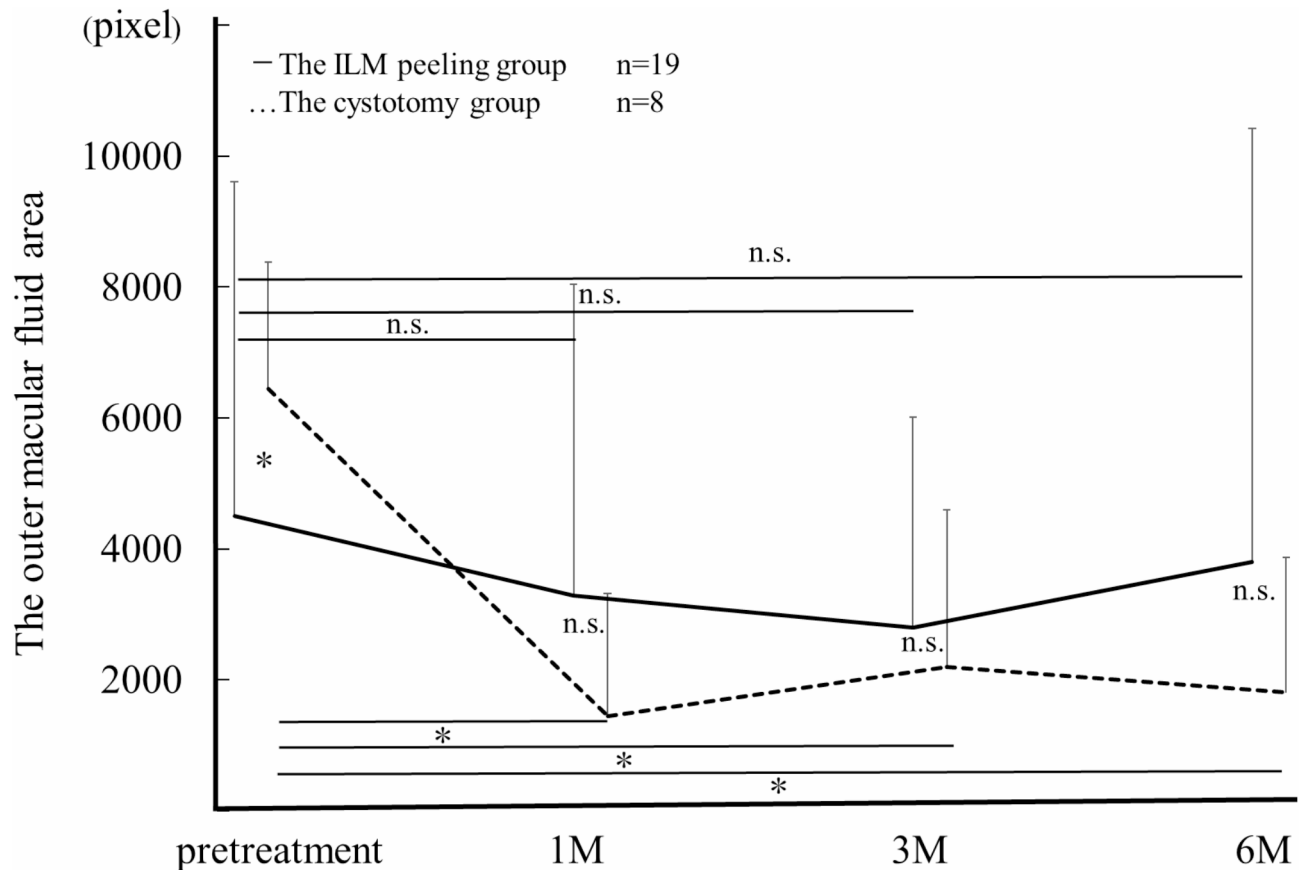


**Fig. 5.** Changes in the area of outer macular fluid at preoperatively and 1, 3, and 6 months postoperatively in the cystotomy groups vs. the ILM peeling groups. n.s.: not significant, \* $P < 0.05$ , Mann-Whitney U test for comparison between groups and Wilcoxon signed-rank test for comparison of time periods in each group.

for cystotomy. One of the reasons for the different patients' treatment backgrounds was that the use of anti-VEGF reagents for DME had not been approved in Japan until 2014. Second, the cystotomy group had fewer eyes than the ILM peeling group because the cystotomy technique is relatively new, so matching the number of cases was difficult. Statistical power analysis to evaluate the reliability of the test results between two groups regarding IMF area showed a beta value of 0.75 in ANOVA, and an increase in the number of cases may lead to significant differences, especially in IMF area. Third, the follow-up period was only one year. To further validate our results on the usefulness of vitrectomy combined with cystotomy, a large prospective controlled study with longer follow-up period is warranted. Finally, the present AI method still has false-positive and false-negative evaluations (Fig. 6), suggesting a potential room for improvement in our model in the future.

In conclusion, the cystotomy group showed a significant reduction in CRT and OMF area postoperatively compared to the ILM peeling group, with preservation of visual acuity and reduction of anti-VEGF treatments. Vitrectomy combined with cystotomy is a valuable treatment option for refractory cystoid DME.

## Methods

### Study subjects

This is a retrospective case-control study. This study followed the principles of the Declaration of Helsinki. The institutional review board in Hokkaido University Hospital (IRB number: C-T2022-0344) approved this study. The IRB at Hokkaido University Hospital approved the study on an opt-out basis, in which patients were given the opportunity to refuse to participate in the study via the website since this is a non-invasive retrospective observational study. Each patient was informed about the risks and benefits of the surgery, and written informed consent was obtained. Thirty-five eyes of 29 patients who underwent pars plana vitrectomy for DME refractory to drug therapy between January 2010 and January 2022 at Hokkaido University Hospital were enrolled in this study. The patients who were not able to be observed for at least 6 months after surgery were excluded. The patients who underwent vitrectomy surgery with cystotomy for ocular fundus diseases other than DME including branch retinal vein occlusion and idiopathic macular telangiectasia were excluded. Eyes of DME patients were divided into 2 groups who underwent vitrectomy surgery with cystotomy (cystotomy group) and those who underwent vitrectomy with ILM peeling only (ILM peeling group).

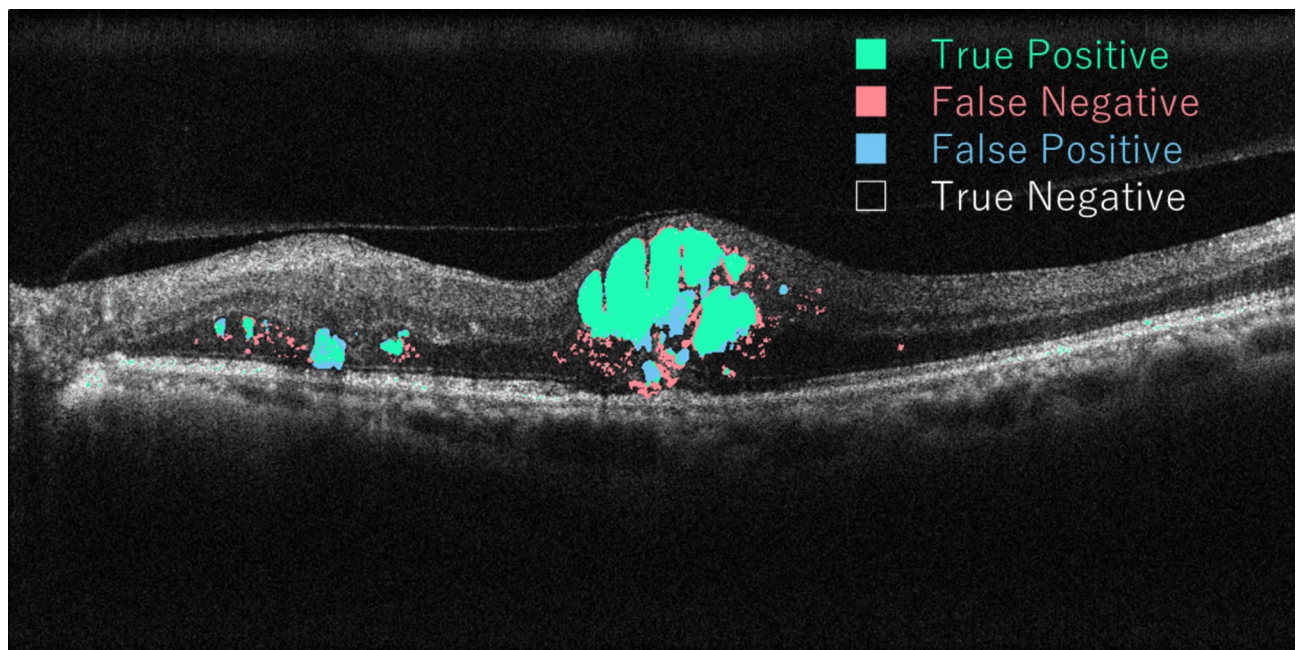


**Fig. 6.** The images of the validation data set to evaluate the accuracy of retinal fluid semantic segmentation.

### Ophthalmic examinations

The medical history of all participants was collected, regarding comprehensive clinical evaluations and ophthalmic examinations, including BCVA, intraocular pressure, slit-lamp microscopy and ocular fundus imaging. All ophthalmic examinations were performed preoperatively and at 1, 3, and 6 months postoperatively for all patients. Swept-source optical coherence tomography (OCT) (DRI OCT Triton or DRI OCT-1 Atlantis; Topcon Inc., Tokyo, Japan) or spectral-domain OCT (RS-3000 or RS-3000 Advance; NIDEK, Gamagori, Japan) was used to examine all eyes preoperatively and at 1, 3, and 6 months postoperatively. CRT in OCT was measured manually from the inner surface of the retinal pigment epithelium to the inner surface of the neurosensory retina at the fovea by one experienced examiner (K.H.). The MF area was calculated using artificial intelligence (AI) on the horizontal scans of the OCT image. The area of MF was subdivided into IMF area bounded by the INL, and OMF area which was the fluid between the outer border of INL and EZ. Analysis of the MF area excluded 8 cases in which OCT images were low in clarity and insufficient for AI analysis.

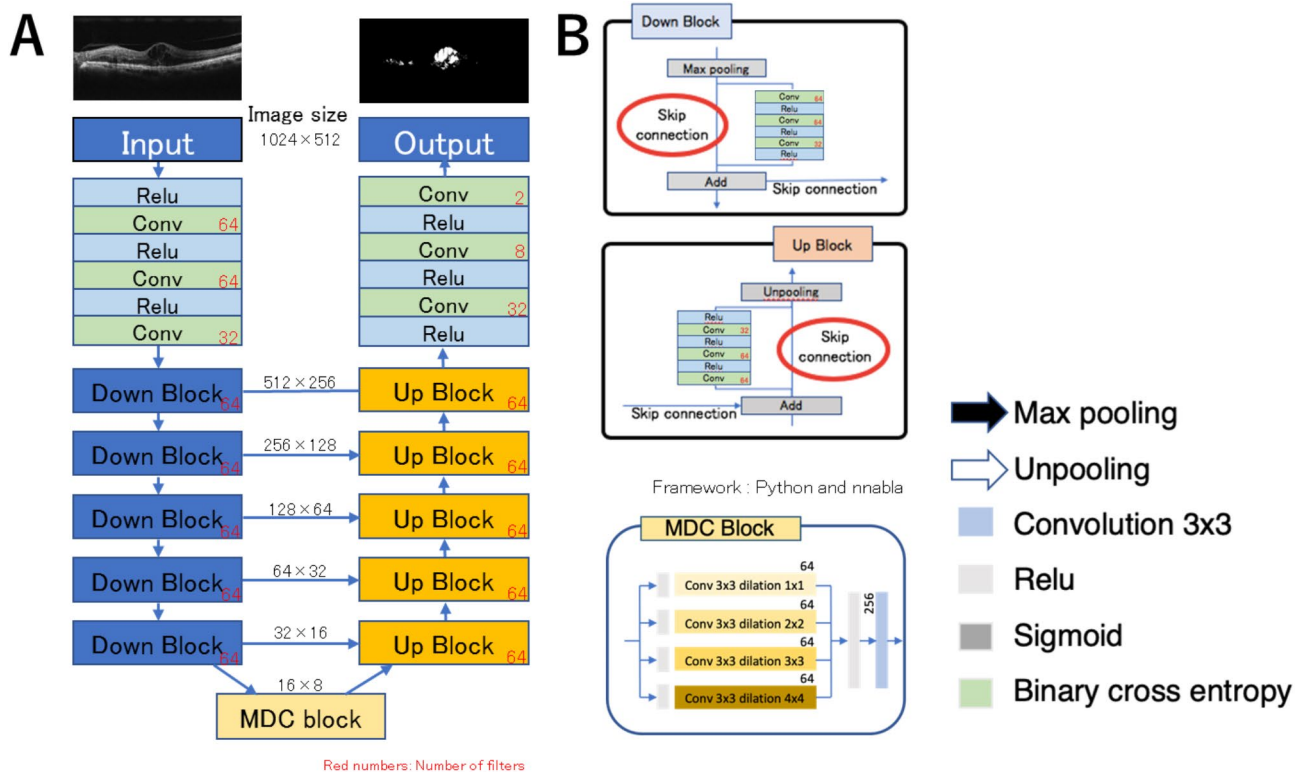
### The neural network for MF segmentation

Figure 7A shows the neural network architecture used in this study. The neural network has an encoder–decoder structure, similar to the U-Net, which is a traditional neural network model used previously for semantic segmentation [20]. A horizontal OCT image with a monochrome channel containing  $1024 \times 512$  pixels is used as an input image. From the 1 deep learning tree, 1 probability map of MF is produced as an output. The probability map is binarized with a threshold set as 205. The threshold value is determined to obtain the maximum AUC value. In Fig. 7A, the blue bars represent Down Block, whereas the orange bars represent the Up Block and multiple dilated convolutional block<sup>21</sup>, respectively. The left-side path consists of repeated Down Blocks connected to the corresponding Up Blocks. The connections are called *skip connections* (Fig. 7B, red circles). In addition to the skip connections between Down Blocks and Up Blocks, each Down Block and Up Block has additional short connections internally, similar to Res Block<sup>22</sup>. The distinct skip connections reduce the gradient loss in backpropagation and solve the vanishing gradient problem as the network becomes deeper. The multiple dilated convolutional blocks consist of 4 dilated convolution layers with different strides. It is placed between the left-side encoder and the right-side decoder, contributing to capturing the global features. Sigmoid function is used to transform the output of the network into a probability map.

### Training methods

We implemented the neural network on NNabla version 1.33.1, (Sony Corporation). Training images were augmented randomly by flipping the images horizontally and rotating them within a 0.26 rad before inputting them into the neural network. To minimize the overhead and use the graphic processing unit memory maximally, we prioritized the size of input images over the batch size. For the NVIDIA A6000 graphic processing unit, we chose original  $1024 \times 512$  square-pixel images and reduced the batch size to 11 samples. The epoch size was set as 1000 with the early stopping method. Binary cross-entropy loss function and Adam optimizer were used with the following parameters: initial learning rate;  $\alpha$ , 0.005;  $\beta_1$ , 0.9;  $\beta_2$ , 0.999; and  $\epsilon$ ,  $1E-8$ .

OCT horizontal images obtained from patients with DME, who visited Hokkaido University Hospital vitreoretina clinic, were used to train and validate the neural network. Four-fifth of the 104 images with DME were used for the training and one-fifth were used for validation of the deep learning system. Training error



**Fig. 7.** Proposed deep learning method. (A) Schematic view of the deep learning model. The numbers written beside each layer represent the number of feature maps, width (pixels)  $\times$  height (pixels). (B) Detailed expositions of the Down Block, Up Block, multiple dilated convolutional (MDC) block, and signs (arrows and layers).

was 0.004668 and validation error was 0.014386, and the learning curves for both the training and validation validators converged and showed no tendency toward overlearning.

### Verification of MF segmentation

In this study, we used a modified deep U-net, which is an improved version of Deep U-Net, a typical neural network used for semantic segmentation. Then, we trained the neural network to generate IMF and OMF probability images from OCT images using our detailed training data. The accuracy of the MF segmentation was evaluated on images from 11 validation datasets (Fig. 6). The accuracy of MF segmentation in the generated segmented images was evaluated by calculating the number of false-positive (FP), false-negative (FN), true-positive (TP), and true-negative (TN) in pixel drawings of MF. Using the parameters, indices to evaluate the accuracy of the deep learning system, such as sensitivity, specificity, overall accuracy, Dice coefficient, and area under the receiver operating characteristic curve (AUC), also were calculated from the equations below: Sensitivity =  $TP / (TP + FN)$ , Specificity =  $TN / (TN + FP)$ , Overall accuracy =  $(TP + TN) / (TP + FP + TN + FN)$ , and Dice coefficient =  $(2 \times TP) / (2 \times TP + FP + FN)$ . The AUC was calculated from sensitivity and specificity using scikit-learn module 0.19.1. using Python version 3.6.4. The validation data used in this method was evaluated to have a sensitivity of 0.767, specificity 0.996, accuracy 0.993, AUC 0.986, and Dice coefficient 0.702. This modified deep U-net, which generates predictive images of IMF and OMF by semantic segmentation from DME OCT images, is named “Hokkaido University macular fluid segmentation model”.

### Surgical techniques

All patients underwent a 25-gauge, transconjunctival pars plana vitrectomy. Patients with cataract underwent a combined procedure with phacoemulsification and aspiration with intraocular lens implantation. Triamcinolone acetonide was used to visualize the vitreous during vitrectomy. After core vitrectomy, the ERM was peeled in the macular region at the discretion of the surgeon in some cases. In the ILM peeling group, the ILM of 2–4 papillary diameters centered on the macula was peeled off and the operation was completed. In the cystotomy group, after removal of the ILM, the upper wall of the cyst was incised with ILM forceps (Supplementary Movie).

### Endpoints

The primary endpoints were CRT, BCVA, and the area of MF preoperatively and at 1, 3, and 6 months postoperatively. The total number of intravitreal injections with anti-VEGF agents and STTA preoperatively and during the 6-month postoperative period were compared between the two groups.

## Statistical analyses

Statistical tests were performed using the R statistical package (version 3.6.1, R Foundation for Statistical Computing). BCVA was measured as decimal values and converted to logMAR units for statistical analysis. The Mann–Whitney U test was used to compare changes in CRT, BCVA, and MF area preoperatively and at 1, 3, and 6 months postoperatively between the two groups. The Wilcoxon signed-rank test was used for changes in CRT, BCVA, and MF area at 1, 3, and 6 months postoperatively compared to preoperatively for each group. ANOVA was performed with CRT and MF area as the dependent variable, and postoperative follow-up time and whether the patient underwent cystotomy or not as independent variables, respectively. The total numbers of intravitreal injections with anti-VEGF agents and STTA preoperatively and during the 6-month postoperative period were analyzed by using the t-test. A  $p$ -value  $< 0.05$  was determined as statistically significant. Data were presented as mean  $\pm$  standard deviation.

## Data availability

All data relevant to the study are included in the article and in the supplementary materials.

Received: 1 May 2024; Accepted: 10 March 2025

Published online: 26 April 2025

## References

- Do, D. V. et al. One-year outcomes of the Da Vinci study of VEGF Trap-Eye in eyes with diabetic macular edema. *Ophthalmology* **119** (8), 1658–1665 (2012).
- Photocoagulation for diabetic macular edema. Early treatment diabetic retinopathy study report number 1. Early treatment diabetic retinopathy study research group. *Arch. Ophthalmol.* **103** (12), 1796–1806 (1985).
- Haller, J. A. et al. Randomized controlled trial of an intravitreal dexamethasone drug delivery system in patients with diabetic macular edema. *Arch. Ophthalmol.* **128** (3), 289–296 (2010).
- Gillies, M. C. et al. Intravitreal triamcinolone for refractory diabetic macular edema: two-year results of a double-masked, placebo-controlled, randomized clinical trial. *Ophthalmology* **113** (9), 1533–1538 (2006).
- Diabetic Retinopathy Clinical Research Network et al. Aflibercept, bevacizumab, or Ranibizumab for diabetic macular edema. *N Engl. J. Med.* **372** (13), 1193–1203 (2015).
- Jackson, T. L. et al. Pars plana vitrectomy for diabetic macular edema: a systematic review, meta-analysis, and synthesis of safety literature. *Retina* **37** (5), 886–895 (2017).
- Christoforidis, J. B. & D'Amico, D. J. Surgical and other treatments of diabetic macular edema: an update. *Int. Ophthalmol. Clin.* **44** (1), 139–160 (2004).
- Massin, P. et al. Optical coherence tomography for evaluating diabetic macular edema before and after vitrectomy. *Am. J. Ophthalmol.* **135**, 169–177 (2003).
- Stefánsson, E. The therapeutic effects of retinal laser treatment and vitrectomy. A theory based on oxygen and vascular physiology. *Acta Ophthalmol. Scand.* **79** (5), 435–440 (2001).
- Kadonosono, K., Itoh, N. & Ohno, S. Perifoveal microcirculation before and after vitrectomy for diabetic cystoid macular edema. *Am. J. Ophthalmol.* **130** (6), 740–744 (2000).
- Tachi, N., Hashimoto, Y. & Oginio, N. Cystotomy for diabetic cystoid macular edema. *Doc. Ophthalmol.* **97** (3–4), 459–463 (1999).
- Imai, H. et al. *Retina* **41**(4):844–851 (2021).
- Asahina, Y. et al. Six-month postoperative outcomes of intraoperative OCT-guided surgical cystotomy for refractory cystoid macular edema in diabetic eyes. *Clin. Ophthalmol.* **11**, 2099–2105 (2017).
- Semeraro, F. et al. Diabetic retinopathy: vascular and inflammatory disease. *J. Diabetes Res.* **2015**, 582060 (2015).
- Cohen, S. R. & Gardner, T. W. Diabetic retinopathy and diabetic macular edema. *Dev. Ophthalmol.* **55**, 137–146 (2016).  
1. 16 kyu20 et al. Photoreceptor function in eyes with macular edema. *Invest. Ophthalmol. Vis. Sci.* **41** (12), 4048–4053 (2000).
- Yanoff, M. et al. Pathology of human cystoid macular edema. *Surv. Ophthalmol.* **28**, 505–511 (1984).
- Imai, H. et al. *Retina* **40**: 154–159 (2020).
- Tanaka, T. et al. Clinicopathological findings in refractory diabetic macular edema-case report. *Biomed. Rep.* **20** (1), 13 (2024).
- Maloca, P. M. et al. Validation of automated artificial intelligence segmentation of optical coherence tomography images. *PLoS One* **14**(8) (2019).
- Yamashita, T., Furukawa, H. & Fujiyoshi, H. Multiple skip connections of dilated convolution network for semantic segmentation. *Proceedings of the 25th IEEE International Conference on Image Processing*. 1593–1597 (2018). (2018).
- He, K., Zhang, X., Ren, S. & Sun, J. Deep residual learning for image recognition. *Proceedings of the IEEE Conference on Computer Vision and Pattern Recognition*. 770–778 (2016). (2016).

## Author contributions

MM wrote the paper and acquired clinical data. MS reviewed the paper and interpreted the clinical data. KH analyzed CRT data. RA, ZD, SK and SI conducted clinical revision and supervised the data interpretation. All authors have read and approved the manuscript.

## Funding

There is no fund received from any organization for this work.

## Declarations

## Competing interests

The authors declare no competing interests.

## Ethical approval

The institutional review board in Hokkaido University Hospital (IRB number:022–0081) approved this study. This study involves human participants with retrospective, non-invasive observations.

## Patient consent for publication

Not required.

## Additional information

**Supplementary Information** The online version contains supplementary material available at <https://doi.org/10.1038/s41598-025-93847-z>.

**Correspondence** and requests for materials should be addressed to M.S.

**Reprints and permissions information** is available at [www.nature.com/reprints](http://www.nature.com/reprints).

**Publisher's note** Springer Nature remains neutral with regard to jurisdictional claims in published maps and institutional affiliations.

**Open Access** This article is licensed under a Creative Commons Attribution-NonCommercial-NoDerivatives 4.0 International License, which permits any non-commercial use, sharing, distribution and reproduction in any medium or format, as long as you give appropriate credit to the original author(s) and the source, provide a link to the Creative Commons licence, and indicate if you modified the licensed material. You do not have permission under this licence to share adapted material derived from this article or parts of it. The images or other third party material in this article are included in the article's Creative Commons licence, unless indicated otherwise in a credit line to the material. If material is not included in the article's Creative Commons licence and your intended use is not permitted by statutory regulation or exceeds the permitted use, you will need to obtain permission directly from the copyright holder. To view a copy of this licence, visit <http://creativecommons.org/licenses/by-nc-nd/4.0/>.

© The Author(s) 2025